Assessing wave climate trends in the Bay of Biscay through an intercomparison of wave hindcasts and reanalysis

F. Paris[1], S. Lecacheux[1], D. Idier[1]

[1] BRGM, 3 Avenue Claude Guillemin Cedex 2, BP 6009, 45060 Orléans, France

Corresponding author: f.paris@brgm.fr

Abstract

The Bay of Biscay is exposed to energetic waves coming from the North Atlantic that have crucial effects on the coast. Thus, to better understand last decade's evolution of coastal hazards and morphology and to anticipate their potential future changes, it is worthwhile to analyze the wave climate trends in this region. This study aims at characterizing the long-term trends of the present wave climate on the second half of the 20th century in the Bay of Biscay through a robust and homogeneous intercomparison of five wave datasets (CERA-40, ERA-INTERIM, BoBWA-10kH, ANEMOC and Bertin and Dodet, 2010).

The comparison of the quality of the datasets against offshore and nearshore buoy measurements reveals that at offshore buoys, global models slightly underestimate wave heights, while regional hindcasts overestimate wave heights, especially for the highest quantiles. At coastal buoys, BoBWA-10kH is the dataset that compares the best with observations. Concerning long time-scale features, the comparison highlights that the main significant trends are similarly presents in the five datasets, especially in summer for which there is an increase of significant wave heights and mean wave periods (up to +15 cm and +0.6 s over the period 1970-2001) as well as a southerly shift of wave directions (around -0.4° y^{-1}). Over the same period, an increase of high quantiles of wave heights during the autumn season (around 3 cm y^{-1} for SWH_{90}) is also noticeable. For winter, significant trends are much lower than for summer and autumn despite a slight increase of wave heights and periods during 1958-2001. These trends have been related to different modifications of the wave types' occurrence.

The results are discussed in terms of comparison with longer time-scale studies and causes of wave climate trends. The future evolutions of wave climates are also broached with the analysis of two wave climate projections (BOBWA-10kF and Morellato et al., 2010).

1 Introduction

The Bay of Biscay (the gulf lying along the western coast of France and the northern coast of Spain, cf. Fig. 1) is exposed to energetic waves coming from the North Atlantic that are created by storm winds and cross the Atlantic Ocean following west-east tracks. These waves have crucial effects on coastal hazards (disturbance, erosion and flooding) and coastal morphology. Therefore, it is worthwhile to better understand wave climate evolution in this region to be able to anticipate its potential future changes and impacts at the coast.

Different types of in-situ data have been used to investigate wave climate trends in the North Atlantic and the Bay of Biscay, from buoy measurements (Dupuis et al., 2006) and Voluntary Observing Ships data (Bacon and Carter, 1991 and 1993) to satellite imagery (Woolf et al., 2002; Izaguirre et al., 2011). However, in-situ measurements do not provide homogeneous records of wave parameters in space and time (buoys are sparsely located and there records present many discontinuities; satellite observations are available since the 90's only) whereas the study of wave climatology and trends requires good quality homogeneous data over long periods with good time and space resolution and coverage. Thus, many efforts have been made in the last decade to produce spatially homogeneous long-time series of wave parameters through wind wave numerical modeling based on global meteorological reanalysis.

Several reanalysis and hindcasts of ocean waves over the second half of the 20th century were produced and analyzed at global scale [ERA-40 and C-ERA-40 for 1958-2001 (Uppala et al., 2005; Caires and Swail, 2004; Caires et al., 2005a and 2005b) ; ERA-INTERIM for 1979-2011 (Dee et al., 2011)] and at regional scale for the North Atlantic [AES40 for 1958-1997 (Swail and Cox, 2000; Wang and Swail, 2004) ; MSC50 for 1954-2010 (Swail et al., 2006)]. In the North Atlantic area, these studies show a general agreement in terms of long-term trends of wave heights: they point out a general increase for latitudes north of 50°N and a decrease south of 40°N. For example, Wang and Swail (2004) and Caires and Swail (2004) highlight a significant increase of winter mean significant wave heights (respectively up to +3 cm y^{-1} and +2.6 cm y^{-1}) in the northeast part of the basin. In the same area, Swail et al. (2006) show similar trends in terms of annual mean significant wave heights (about +0.6 cm y^{-1}). Even so, in the intermediate area of the Bay of Biscay (between 40°N and 50°N), no significant changes are detected in these studies, whatever the dataset and the season. However, the spatial resolutions of global wave models (1.5° for ERA-40) or North Atlantic models (0.625° in latitude by

0.833° in longitude for AES40) are insufficient to analyze properly this intermediate region, for which the wave height trends have a poor significance.

To date, three regional long-term wave hindcasts are available for the area of the Bay of Biscay: ANEMOC, covering the French Atlantic coasts, the English Channel and the North Sea over the period 1979-2002 (Benoit and Lafon, 2004); BOBWA-10kH, generated with a dynamical downscaling from the North Atlantic to the Bay of Biscay over the period 1958-2002 (Charles et al., 2012a); and the wave hindcast generated by Dodet et al. (2010) over the period 1953-2009. The comparison of the long-term trends highlighted by these studies is not straightforward because the periods investigated and the methods employed differ from one author to another. On the period 1953-2009, Dodet et al. (2010) show an increase of significant wave heights up to 2 cm y^{-1}, a slight increase of annual peak period of about 0.01 s y^{-1} and a clockwise rotation (i.e. a northerly shift) of mean wave direction ranging from 0 to 0.05° y^{-1}. Nevertheless, the significance of these trends is not given by Dodet et al. (2010), whereas Charles et al. (2012a) doesn’t point out any significant trend for the same period. In contrast, for the period 1970-2001, Charles et al. (2012a) highlight a significant increase in summer wave heights (0.5 cm y^{-1} for mean significant wave heights, and 2.6 cm y^{-1} for the 90th quantile at the Biscay Buoy) as well as a northerly shift of wave directions during spring and a southerly shift during autumn.

To sum up, the results of these studies are not contradictory, but some discrepancies limit the comparison between the datasets, and thus their use to provide robust trend information: the parameters (seasonal or annual means, 90th or 95th quantiles), the time period, the geographic area, the use of the statistical significance test, etc. Therefore, this paper aims at characterizing the trends of the present wave climate in the Bay of Biscay, by re-examining the conclusions of the above-mentioned studies through a robust and homogeneous intercomparison of different raw datasets. For that purpose, we selected the three available regional wave hindcasts in the Bay of Biscay but also the global wave reanalysis C-ERA-40 and ERA-INTERIM. Indeed, even if the resolution of global models is limited, the use of these two reanalysis enables to enrich the restricted number of regional datasets and to take into account reanalyzed wave data (that have been corrected through data assimilation using wave observations). Although our main goal is to compare wave trends in the different hindcasts and reanalysis, the quality of the different datasets has to be estimated first. This is done by using buoy measurements along the French coast. Then, the seasonal trends of mean significant wave heights (SWH), 90th quantile of significant wave heights (SWH_{90}), mean wave periods (MWP) and mean wave directions (MWD) can be estimated based in the datasets results comparison, and for different time periods.

The paper is organized as follows. Section 2 describes the selected reanalysis and hindcasts and details the methodology applied for the comparison of the datasets quality and trends. In the two following sections, we present the results of the quality analysis (Sect. 3) and the long-time scale features assessment (Sect. 4). Section 5 is dedicated to the discussion and the conclusion is drawn in Sect. 6.

2 Data and method

2.1 Wave datasets description

The characteristics of the five datasets are synthetized in Tab. 1 and a detailed description (grids, resolutions, wind data, wave models, validation, calibration data and method, etc.) is provided in the following five sections. The positions of the buoys used for the calibration or the validation of the different datasets (and situated in our study area) are showed on Fig. 1.

2.1.1 C-ERA-40

ERA-40 (Uppala et al., 2005) is a 40-year (1957–2002) world climatology reanalysis produced by the European Centre for Medium-Range Weather Forecasts (ECMWF) based on an atmospheric model coupled with the wave model WAM (Komen et al., 1994). It benefits from the assimilation of altimeter measurements (like ERS-1 and ERS-2 from 1992 to 2001) and was validated against buoy measurements. As some inhomogeneities were introduced by the use of different altimeter data, Caires and Sterl (2005a and 2005b) corrected the SWH with a nonparametric regression method and provided the new 45-yr global 6-hourly dataset C-ERA-40. The wave fields are provided every 6 hours on a 1.5° grid.

2.1.2 ERA-INTERIM

ERA-Interim (Dee et al. 2011) is the latest global atmospheric and oceanographic reanalysis produced by the ECMWF covering the time period from 1979 to 2011. Amongst others, the project was conducted to prepare the new atmospheric reanalysis ERA-CLIM covering the 20th century. Built on the experience acquired with ERA-40, ERA-INTERIM benefits from improved data assimilation systems (ERS-1 and ERS-2 satellite observations have been corrected, and ENVISAT, JASON-1 and JASON-2 data have been added) and numerical models. The wave data are provided every 3 h on a 0.7° resolution grid

2.1.3 ANEMOC

ANEMOC (Digital Atlas of State Oceanic and Coastal Sea; Benoit and Lafon, 2004) is a wave hindcast covering the French Atlantic coasts, the English Channel and the North Sea over a period of 23 years (1979-2002). It has been built with the TELEMAC-based Operational Model Addressing Wave Action Computation (TOMAWAC; Benoit et al., 1996) and the 6 hourly ERA-40 wind fields. The spatial resolution of the wave model ranges from 1° offshore to 2-3 km near the coast. Validation was carried out on 4 buoys along the French Atlantic coast (Yeu, Ouessant, Minquiers and Le Havre) over a period of 2 years (1999-2000). The wave parameters are provided every hour on different points over the Bay of Biscay. In our study, these data have been interpolated on a 0.1° grid resolution to produce gridded wave fields.

2.1.4 BAD

Dodet et al. (2010) produced a 57–year wave hindcast (1953-2009), covering the North Atlantic Ocean with a resolution of 0.5°. The simulations were realized with the version 3.14 of the third-generation spectral wave model WAVEWATCH III™ (WW3) (Tolman, 2009), the parameterization of Ardhuin et al. (2009a, 2009b) and the 6 hourly wind fields from the NCEP/NCAR Reanalysis (Kalnay et al., 1996). The validation against buoys measurements (five buoys along the Portuguese coast plus one along the Spanish coast) pointed out an underestimation of the simulated SWH (systematic bias from -0.10 m to -0.30 m). Thus, Bertin and Dodet (2010) produced a new wave hindcast based on the same model but forced with 3% increased NCEP/NCAR wind fields to correct this negative bias. Besides, a 0.2° grid centred on the Bay of Biscay and the English Channel was added to provide higher resolution data on the French Atlantic coasts. The validation of the second grid, carried out against four buoys situated in our study area (Saint-Yves, Cap-Ferret, Bilbao and Bares), showed lower statistical errors than the previous dataset. For this reason, we chose to use this corrected dataset, hereafter called BAD, which provides wave fields every 6 hours on the 0.2° grid.

2.1.5 BOBWA-10kH

BOBWA-10kH (Charles et al. 2012a) is a property of BRGM and CNRM-GAME (URA1357; CNRS-Météo-France). It is a wave hindcast covering the period 1958-2001 for the North Atlantic (spatial resolution of 0.5°) and the French Atlantic and English Channel coasts (spatial resolution of 0.1°). It was produced with a two-way nested WW3 (Tolman, 2009) modelling framework using the TEST441 source terms parameterization (Ardhuin et al., 2010). The model was forced by the ERA-40 wind fields (Uppala et al. 2005) given every 6h at a height of 10 m on a 1.125° x 1.125° grid. A calibration was carried out by varying the wind input height and comparing the simulated waves against the Biscay buoy measurements on the period 1998-2002. The optimal altitude value was assigned at 4.5m. The dataset was also validated against 7 buoys (Biscarrosse, Cap-Ferret, Saint-Nazaire, Minquiers, Cayeux, Yeu1 et Yeu 2) over the period 1998-2002. The results are available every 6 hours for each point of the 0.1° grid.

2.2 Wave climatology in the Bay of Biscay

A first investigation is carried out to describe the wave climatology and identify the spatial and seasonal variability in the region of the Bay of Biscay (10°W-0°E; 43°N-52°N). To this end, we use the maps of mean wave parameters (SWH, SWH_{90}, MWP and MWD) derived from BOBWA-10kH for the period 1979-2001 (Fig. 2). Generally speaking, annual mean SWH values vary spatially, decreasing from the open sea (about 3 m at 10°W) to the coast (1 m along the South French coast). In spring and autumn, seasonal means of SWH are of the same order of magnitude (from 3 m at 10°W to 1.5 m at 1°W), whereas they are larger in winter (from 5 m at 10°W to 2 m at 1°W) and lower in summer (from 2 m at 10°W to 1 m at 1°W). SWH_{90} show similar patterns but with larger values (from 7 m at 10°W to 3.5 m at 1°W during winter). Concerning the mean wave period (MWP), a much more regular seasonality is observed, with summers characterized by MWP of about 7 s and winter MWP ranging from 10 s to 11 s. A slight gradient from +0.5 s to +1 s appears from North (51°N) to South (44°N). Finally, we can observe that annual and seasonal averaged waves come from almost the same direction, i.e. from the west-north-west (from 280°N at 51°N to 300°N at 44°N).

As a preliminary intercomparison, the analysis of the other datasets (maps not shown) reveals that the three hindcasts and two reanalysis exhibit the same patterns in the study area. Concerning the annual and seasonal means of SWH, the three regional datasets (ANEMOC, BAD and BOBWA) are very comparable in terms of spatial variability and range of values.

Nevertheless, BAD and ANEMOC show higher means for SWH_{90} (+5 % and + 10 % respectively). For the two global reanalysis, we notice a good similarity in terms of variability, but their seasonal means of SWH are lower than those of the three regional hindcasts (from -10 % to -15 %). For the mean wave period (MWP), BAD and BOBWA show similar values within the Bay of Biscay but the three other datasets (C-ERA-40, ERA-INTERIM and ANEMOC) present lower means (between -10% to -25%). In terms of mean wave direction (MWD), we do not observe any significant differences between the datasets.

2.3 Method of intercomparison

The intercomparison of the datasets contains two steps: first, the assessment of the quality of each dataset and second, the comparison of long-term trends.

For the first step, the models outputs (SWH, SWH_{90}, MWP and MWD) are compared against five buoy measurements spread over the study area (cf. Fig. 1): two offshore buoys [Brittany (2100 m depth) in the North Atlantic and Biscay Buoy in the Bay of Biscay (4500 m depth)] and three coastal buoys along the French coast [Biscarrosse (26 m depth), Yeu (35 m depth) and Minquiers (38 m depth)]. Although our study focuses on the Bay of Biscay, the three regional models also cover the English Channel. Thus, we decided to include the Minquiers buoy in this section to investigate the limitations of the models in this area. It is worth mentioning that models outputs correspond to grid nodes and thus do not always match exactly buoy locations, especially for global datasets. In order to homogenize the datasets, the squared 6 hourly mean significant wave heights and periods and the 6 hourly mean wave directions are calculated for each dataset and each buoy record. The 6-hourly fields from these 5 buoys locations are analyzed through different plots, such as scatter and quantile-quantile plots (Q-Q plots, see Fig. 3b for example) which show the correspondence between measured and computed quantiles (from 1% to 99%) of the statistical distribution of SWH. These plots allow analyzing model capacity to fairly reproduce both weak and energetic waves with a similar accuracy. The differences between models outputs and observations are also quantified by computing standard statistics: the systematic deviation between two random variables (BIAS, Eq. 1), the root mean square error (RMSE, Eq. 2), the residual scatter index measuring the dispersion with respect to the line x=y (SI, Eq. 3), and the coefficient of determination, known as the square of Pearson’s correlation coefficient (R^2, Eq. 4).

$$BIAS = \overline{y} - \overline{x} \quad (1)$$

$$RMSE = \sqrt{\sum_{i=1}^{n} (y_i - x_i)^2 \Big/ n} \quad (2)$$

$$SI = RMSE \Big/ \overline{x} \quad (3)$$

$$R^2 = \sum_{i=1}^{n} (y_i - \overline{x})^2 \Big/ \sum_{i=1}^{n} (x_i - \overline{x})^2 \quad (4)$$

with x, representing the observations, y, the wave model data, and n, the number of observations. These statistics are synthesized in Taylor diagrams (Taylor, 2001) which provide a convenient way to represent multiple statistical metrics of model-data comparisons on the same plot (see Fig. 3a for example).

For the second step, we carry out a comparison of seasonal trends in the region of the Bay of Biscay (10°W-0°E; 43°N-52°N). Here, the four meteorological seasons are defined as DJF (December-January-February), MAM (March-April-May), JJA (June-July-August) and SON (September-October-November). For a detailed analysis of trends, we analyze simultaneously (1) the surface plots for the variables SWH, SWH_{90}, MWP and MWD (ex.: Fig. 7), and (2) the bivariate diagrams of wave densities (distribution of significant wave heights against mean wave periods or directions) on local points (ex.: Fig. 8).

The surface plots are based on reconstructed 6-hourly squared means of significant wave heights and mean periods and 6-hourly mean directions at each cell of the grids. Seasonal mean as well as normalized standard deviation (%) and trends of wave parameters are then computed. The significance of the trends is indicated on each plot by the p-value of the Student's T-Test (Student, 1980). Usually, trends are considered significant when the p-value is less than 0.05 but we show the entire plots in order not to restrict the analysis to the most significant areas. Trends significant at more than 95% (probability value < 0.05 on the map) are indicated by hatching on the trend maps (ex.: Fig. 7).

The bivariate diagrams are elaborated such as in Charles et al. (2012a) by dividing the 2D space into cells of 1 m (for SWH) and 1.25 s (for MWP) or into cells of 1 m (for SWH) and 18° (for MWD) and calculating the percentage of events in each cell. They enable to assess the repartition of the types of waves, from wind-seas to swells. To better distinguish the different types, the median steepness is also plotted. With their analysis at the Biscay Buoy, Butel et al. (2002) and Le Cozannet et al. (2011) estimate that the waves above this curve can be considered as swell and the waves below represent a mix of swell and wind-seas (intermediate waves). More details about this method are given in Le Cozannet et al. (2011) and Charles et al. (2012a). For the analysis, models outputs are extracted at two locations corresponding to coastal buoys positions at different latitudes (see Fig. 1): Ouessant (48°N) and Cap-Ferret (44.65°N). For the global models, the coarse spatial resolution induces a higher distance between the extraction point and the real buoys locations. As these two buoys are close to the coast (Ouessant at 45 km and Cap-Ferret at 15 km) and as global models do not take into account nearshore processes, the diagrams done for global models should be considered as tools to study the trends rather than an accurate representation of the reality.

3 Quality of the datasets

The comparison of the datasets against buoy measurements is performed on the 5 buoys described in Sect. 2 and Fig. 1. The quality of the regional models is investigated at every buoy but the global models are analysed only for the two offshore buoys (Brittany and Biscay). Table 2 provides the number of measurements (n), the correlation coefficient (R^2), the bias (BIAS), the Root mean square error (RMSE) and the scatter Index (SI) of the five SWH and MPW datasets for each buoy. In the following, we analyse successively the quality of the datasets for SWH, MWP and MWD through these statistics, the Q-Q plots and the Taylor diagrams.

3.1 Significant wave height

Figure 3 presents several graphics synthetizing the statistics of the five SWH datasets against the two offshore buoys measurements (Brittany and Biscay). The Q-Q plots are showed only for the Brittany buoy but the Taylor diagram gathers the statistics of both buoys. At the Brittany buoy, we notice on Tab. 2 that the global models tend to underestimate wave heights (negative bias down to -19 cm for C-ERA-40) whereas the regional models tend to overestimate (positive bias from +9 cm for BOBWA-10kH to +22 cm for BAD). Q-Q plots for the Brittany buoy (Fig. 3b) show that if the regional models tend to overestimate wave heights above 3-4 m, the underestimation of global models begins for higher quantiles (above 8 m). At the Biscay buoy (Q-Q plots not shown), the same type of behaviours is observed but (1) the underestimation of global models is more pronounced for lower waves (above 3–4 m) and (2) the overestimation of regional models concerns only the highest quantiles (above 5 m for BAD and above 7 m for BOBWA-10kH and ANEMOC). As shown by the statistics summarized on the Taylor diagram (Fig. 3a), ERA-INTERIM and BOBWA-10kH are the two models that compare the best with offshore buoy observations (ERA-INTERIM is of superior quality at Brittany buoy but BOBWA-10kH compares better with observations at the Biscay buoy).

Concerning the coastal buoys (Yeu, Biscarrosse and Minquiers), the detailed results for the three regional datasets are provided on Fig. 4. As for the offshore buoys, the Taylor diagram (Fig. 4a) presents the statistics at each buoy but the Q-Q plots concern only the Yeu buoy. At the Yeu buoy, the comparative statistics of the datasets synthetized on Tab. 2 are very similar, although BOBWA-10kH shows slightly lower errors. For the highest quantiles, the Q-Q plots (Fig. 4b) show that ANEMOC and BAD tend to overestimate wave heights (error beyond +10%) when BOBWA-10kH tend to underestimate (between -5% and -10%). At the Biscarrosse buoy (Q-Q plots not shown), all the models tend to strongly overestimate all type of waves and show positive bias between +0.11 m (BOBWA-10kH) and +0.26 m (ANEMOC). This phenomenon could be explained by the proximity of the coast (~5 km) and the limited resolution of the regional models in this area (around 0.1°) that does not allow simulating properly the nearshore wave transformations. At the Minquiers buoy (Q-Q plots not shown), we could have expected a poorer quality of the models (because none of the models take into account the interaction with the strong tide – water level and currents - in this area) but the statistical errors are of the same order of magnitude than those at the Yeu buoy. Nevertheless, Charles et al. (2012a) showed that even if the statistics of BOBWA-10kH at the Minquiers buoy are comparable with those of the Atlantic buoys, the results obtained for more eastern buoys (like Cayeux and Dunkerque, not investigated in this study) differ considerably with larger biases and RMSE. Even though, there is a systematic underestimation of wave heights for all the quantiles ranges at this buoy (with bias from -0.09 m for BOBWA-10kH to -0.25m for ANEMOC). To sum up, statistical errors of BOBWA-10kH at the three selected coastal buoys are generally lower than those of ANEMOC and BAD (cf. Taylor diagram, Fig. 4a).

3.2 Mean wave period and direction

The analysis of MWP quality is based on Tab. 2 summarizing the statistic errors for each dataset. In general, the quality of the datasets is better on offshore buoys (with R^2 above 0.8) than on coastal buoys (with R^2 between 0.5 and 0.8). Contrary to the analysis of SWH for the offshore buoys (Brittany and Biscay), there is no distinct behaviours for global models on the one hand and for regional models on the other hand and there is no evidence that one of the datasets produces MWP of higher quality. For the coastal buoys (Biscarrosse, Yeu and Minquiers), all the regional models tend to overestimate wave periods (except ANEMOC and

BAD at Yeu buoy) but BOBWA-10kH compares slightly better with observations for most of the buoys.

Concerning the directions, only two of the selected buoys (Yeu on the Atlantic coast and Minquiers in the English Channel) provide records of wave directions in our study area. Thus, the analysis is based on two graphics representing the repartition of the directions of the three regional models at the two buoys (Fig. 5). If the main direction of waves (corresponding to swells) is accurately reproduced by the three models at Yeu buoy (around 270°), the differences are much larger at Minquiers buoy. BAD and BoBWA-10kH well reproduce the main direction (280° to 300°) whereas ANEMOC shows a deviation of about 30° north comparing to observations. This could be explained by the fact that tide and tidal currents (particularly pronounced in the English Channel) are not taken into account in the different wave models. As suggested in Charles et al. (2012a), tide's influence in the Channel grows up from west to east and it is likely that wave directions have a poorer quality further in the English Channel in BAD and BoBWA-10k datasets. Lastly, for both buoys, the comparison with observations highlights some weaknesses in the reproduction of other directions (corresponding to wind-seas), probably due to the coarse discretization of directions in the models and the wind dataset quality.

3.3 Summary and analysis

To summarize, at offshore buoys, global models slightly underestimate wave heights, while regional models overestimate wave heights, especially for the highest quantiles. In general, BOBWA-10kH compares better with observations than the other regional datasets in terms of standard statistical errors. For coastal locations, BOBWA-10kH represents best the wave heights measurements as the two other regionals models (ANEMOC and BAD) tend to over-estimate the highest wave heights. For all datasets and all locations, mean wave periods are poorly reproduced. Concerning wave directions, a deviation of the main direction of about 30° north regarding to measurements is observed in the English Channel for the ANEMOC model.

The determination of the effect of the model specificities (spatiotemporal resolution, physical equations, wind forcing, calibration methods, etc.) on the quality of the datasets is not straightforward. If the low spatiotemporal resolution of the global reanalysis can account for the underestimation of wave heights, it is harder to explain the differences between the regional hindcasts. Among them, BOBWA-10kH and BAD are based on the same wave model (WW3), and ANEMOC and BOBWA-10kH are forced with the same wind field (ERA-40). However, at the selected buoys, we did not notice more similarities between ANEMOC and BOBWA-10kH or between BAD and BOBWA-10kH. The calibration method and the data used for the calibration seem to have more impact on the quality of a dataset than the wave models and the raw wind data used to force it. Finally, as the quality of the datasets is often optimum in the areas of calibration, it is logical to observe a spatial variability in the quality of the datasets and the good quality of BOBWA-10kH in the Bay of Biscay can be explained by the choice of the Biscay buoy for the calibration. It is more than likely that BAD quality is better along Spanish and Portuguese coasts.

It is worth mentioning that our comparison concerns mean wave parameters and does not consider the analysis of the different types of waves and extremes. Besides, as the objective of the study is to analyze wave trends, we focused only on long-term hindcasts and reanalysis. Yet, other datasets with higher spatial and temporal resolutions are available such as IOWAGA (Magne et al., 2010). Even if they cover a shorter time period, these datasets may be more accurate to reproduce historical events such as storms.

4 Long time-scale features

Based on the periods covered by the datasets and the trend study of Charles et al. (2012a), three time periods can be identified: 1958-2001 which is the longest available period, 1979-2001 which is common to the five datasets, and 1970-2001 for which the strongest significant trends were observed by Charles et al. (2012a). However, no significant trend appeared for 1979-2001. For example, summer trends of SWH for the period 1979-2001 are illustrated on Figure 6. Even if the SWH positive trend is of the same order of magnitude in the five datasets (+0.5 cm y^{-1} to +1 cm y^{-1}), it is not significant enough to be highlighted. Thus, we focus on time frames 1958-2001 and 1970-2001, which exclude the use of ANEMOC and ERA-INTERIM since these datasets starts in 1979. In the following, the used datasets are C-ERA-40, BAD and BOBWA-10kH.

In the following, we analyse both the linear trends of wave parameters on the surface plots and the linear trends of wave type distribution on the local bivariate diagrams. Only the significant trends (p-value lower than 0.05) common to all datasets are described and illustrated. The results are organized season by season from summer to winter. Spring is not developed because no significant trend common to the datasets was highlighted for this season.

4.1 Summer

Summer is characterised by the most significant and largest trends and the strongest similarity between the datasets, especially for the period 1970-2001 (Fig. 7).

The detailed analysis of the seasonal maps enabled to point out a significant increase of wave height for the whole French Atlantic coast during the period 1970-2001 in the three available datasets (C-ERA-40, BAD and BOBWA-10kH). This increase ranges from +0.5 cm y^{-1} to +1 cm y^{-1} for SWH and from +0.5 cm y^{-1} to +2 cm y^{-1} for SWH_{90}. For the same period, there is also a slight significant increase of the mean wave period in the whole grid which is more pronounced in C-ERA-40 (up to +0.04 s y^{-1}) than in BAD and BOBWA-10kH (up to +0.02 s y^{-1}). Concerning wave directions, we notice a significant southerly shift in the three datasets particularly pronounced north of 48°N (between -0.2° y^{-1} and -0.4° y^{-1} in the area bordered by the French Brittany Peninsula and the Celtic sea). Over the period 1958-2001 (map not presented), the positive trend of the mean period highlighted for 1970-2001 is still noticeable but in the southern part of the grid only (under the 48°N latitude).

The analysis of the bivariate diagrams for the period 1970-2001 enables to partly explain these trends. Figure 8 shows an extract of the bivariate diagrams for Ouessant and Cap-Ferret buoys. The diagrams SWH/MWP exhibit, for the three datasets and the two buoys, a significant increase of the relative occurrence of energetic waves with heights above the 90^{th} quantile and periods above 6 s. For C-ERA-40 only, there is a significant increase of lower waves (under 2m) with high periods corresponding to the swell type (with a low steepness). Concerning the diagrams SWH/MWD, they show a significant increase of the highest waves whose directions range between 250° and 300°.

4.2 Autumn

For this season, the significant wave height is the only variable showing consistent trends in the various datasets (see Fig. 9). As for the summer, this trend is positive and stronger for the period 1970-2001. For SWH, this increase is significant only for C-ERA-40 and BAD with values up to +1.5 cm y^{-1}. For SWH_{90} (map not shown), it is significant for the three datasets but more pronounced in C-ERA-40 and BAD for which it reaches +3 cm y^{-1} in the northern part of the grid (north of 48°N, in the Celtic sea and the English Channel). The period 1958-2001 is also characterised by a slight significant increase of SWH_{90} in the three datasets (about 0.5-1 cm y^{-1}) but only above 48°N.

The analysis of the bivariate diagrams SWH/MWP for the period 1970-2001 (Fig. 10, left) shows a significant increase of waves of intermediate type (with higher heights but no higher periods). In C-ERA-40 and BAD, this increase is more pronounced for waves above the 90th quantile whereas it is noticeable only for waves below the 90th quantile in BOBWA-10kH. This could explain the differences between the datasets observed in the surface plots of SWH and SWH_{90}. Concerning the diagrams SWH/MWD (Fig. 10, right), they also highlight an increase of the highest waves but no particular trend for the directions.

4.3 Winter

In winter, there is a general increase of wave heights in the three datasets for both 1970-2001 and 1958-2001, particularly above the French Brittany Peninsula. In this area, BAD and C-ERA-40 show a significant trend of SWH_{90} up to +2 cm y^{-1} for 1970-2001 and up to +1.5 cm y^{-1} for 1958-2001 (cf. Fig. 11, top). For BOBWA-10kH, this trend is of the same order of magnitude but it is less widespread and not significant (although the significance is above 80%). A slight increase of wave periods (+0.02 s y^{-1} to +0.04 s y^{-1}) is also detectable in the three datasets for the period 1958-2001, more particularly along the Aquitaine coast (cf. Fig. 10, bottom). For the directions, none of the datasets present any trend.

Bivariate diagrams SWH/MWP (Fig. 11, left) exhibit two different patterns at the Ouessant buoy (in front of the French Brittany Peninsula) and the Cap-Ferret buoy (situated near the Aquitaine coast). At the Cap-Ferret buoy, there is an increase of longer waves occurrence but no particular increase of wave heights whereas at Ouessant buoy, there is an increase of energetic waves with longer periods and higher waves. It explains the spatial differences in latitude observed on the maps (Fig. 10). On the contrary, the same pattern appears for both locations on the SWH/MWD diagrams (Fig. 11, right) as we notice an increase of waves whose direction ranges between 280° and 300°.

4.4 Summary and analysis

Despite the discrepancies between the datasets observed in the quality analysis (Sect. 3), the comparison of long-term features derived from the three datasets C-ERA-40, BOBWA-10kH and BAD, enabled to highlight common trends. More particularly, some similarities have been brought to light during the period 1970-2001 which was not investigated by all the authors. To summarise our findings:

- No significant trend is pointed out for the spring season.
- For the summer season, the comparison highlighted a strong similarity between the trends of wave parameters and wave distributions of the datasets C-ERA-40, BAD and BOBWA-10kH for the period 1970-2001. For this period, the analysis of maps and local points pointed out a general increase of wave heights (+15 cm for mean SWH and +60 cm for the 10% highest SWH) and periods (+0.6 s) with a southerly shift of wave directions (-1°) in the three datasets that can be partly explained by an increase of the occurrence of more energetic waves (with heights above the 90th quantile and high periods) from the west-north-west (between 250° and 300°).
- In autumn, an increase of the wave heights above the 90th quantile is still noticeable in the three datasets (although more pronounced for C-ERA-40 and BAD) for the period 1970-2001 (up to +45 cm for SWH and up to +90 cm for SWH_{90} north of 48°N). It can be explained by an increase of the occurrence of waves with higher steepness (with higher heights but no particular change for the periods).
- Even if the trends are less significant than in summer, the winter season is also characterized by a general increase of wave heights for both 1970-2001 and 1958-2001 (particularly north of the Brittany Peninsula) and mean wave periods for 1958-2001 (particularly south of the Brittany Peninsula). The analysis of bivariate diagrams showed that it could be partly explained by an increase of energetic waves coming from the west-north-west (between 280° and 300°) but whose characteristics vary depending on the latitude. In the northern part of the bay, they are characterized by larger heights and periods and in the southern part of the bay they are characterized by longer periods only.

Thus, a general increase of wave heights is detected at the end of the 20th century for summer, winter and autumn seasons. Although, the analysis of bivariate diagrams enables to point out that this increase is not due to the same mechanisms and type of waves depending on the season.

As for the quality analysis, the explanation of the similarities between trends from different datasets is not straightforward. One can suppose that the wind data used to force the wave models are determining but we did not clearly notice more similarities between BOBWA-10kH and C-ERA-40 (which are derived from the same source of wind).

5 Discussion

5.1 Comparison with longer time-scale studies

In this study, we investigated the long-term trends of wave parameters over the second part of the 20^{th} century. At longer time scale, two studies explored wave climate evolution in the North Atlantic over the entire 20^{th} century based on statistical (Wang et al., 2012) or dynamical (Bertin et al., 2013) reconstruction of SWH from the 20^{th} Century atmospheric Reanalysis (20CR, Compo et al., 2011). They both show an increase of annual SWH over the 20^{th} century in the northern part of the basin and in the Bay of Biscay even if the spatial patterns and order of magnitude of this trend differ from one study to another (the detailed comparison is difficult due to the use of different variables). Wang et al. (2012) also show that the trends magnitudes vary depending on the season (with higher magnitude in summer) and the period analysed (stronger trends are detected for the second half of the 20^{th} century). Even though, present trends of SWH detected in this study seem to follow SWH trends over the 20^{th} century.

5.2 Causes for SWH trends

Several studies investigated the causes of SWH trends in North Atlantic, from inter-annual variability (partly-controlled by the NAO oscillation) to long-term trends in North Atlantic winds and storminess.

Fig. 13 presents the inter-annual variations of SWH at the Biscay buoy for each dataset used in this study as well as the annual NAO index. Whatever the season, inter-annual variability of SWH is very strong (from 0.25 m in summer to 2 m in winter) and the variations followed by the datasets over the years are very similar. As demonstrated in previous studies (Kushnir et al., 1997; Wang and Swail., 2001 and 2002; Dodet el al., 2010; Charles et al., 2012a), these inter-annual variations can be partly related to the NAO index (NAO+ being characterized by stronger and northerly shifted winds in the North Atlantic). In particular, Charles et al. (2012a) point out that NAO+ is correlated with an increase of wave heights and periods during winter and a decrease of wave heights during summer associated with a northerly shift of wave directions for both seasons. Thus, if the increase of NAO+ occurrence over the second part of the 20^{th} century can help understanding winter wave height increase detected in the datasets studied in this paper, the link with summer wave heights increase is more difficult to interpret.

Another approach entails relating changes of wave characteristics to long-term changes of wind fields in the North Atlantic Ocean. Some recent studies have pointed out an increase in wind speed over the past 25 years (Young et al. 2011), and also an increase of annual storm occurrence for the northern and western Europe since 1960 with a peak of storminess near the early 90' (Donat et al., 2011). However, storminess variability and trends over the European regions exhibit high regional and seasonal differences (Wang et al., 2009 and 2011). Through an analysis of inland surface pressure observations since 1878, Wang et al. (2009, 2011) notably show that the peak of storminess detected at the end of the 19th and the 20th century did not occur at the same season (winter or summer) depending on the regions and the latitudes. Thus, a thorough analysis of seasonal storminess variability and trends over the entire North Atlantic Ocean could help understanding the mechanisms at stake and explaining the seasonal differences in wave climate trends detected in this study.

5.3 Future evolution of these trends

The studies investigating the future wave climates are more recent and only a few of them concerns the Bay of Biscay. Among the datasets used in our study, two were extended on the period 2061-2100 under climate change scenarios (A2, A1B and B1): (1) Charles et al. (2012b) produced the wave forecast BOBWA-10kF with the same model as BOBWA-10kH and wind fields from the RETIC simulations of ARPEGE-Climat (Gibelin and Déqué, 2003) (2) Morellato et al. (2010) produced a wave forecast with the same model as ANEMOC and the wind fields ECHAM5/MPIOM. The examination of wave climate changes (performed with a similar approach as for the present trends, see Sect. 2.3) points out that past trends do not pursue, as we observe a general decrease of wave heights between the end of the 20th and the 21th centuries in both datasets. This decrease is all the more pronounced for the more pessimistic scenarios (from B1 to A2). As for present trends, summer is the season for which the largest changes are observed with a decrease of -12% of SWH and a clockwise shift of +8% of MWD at Brittany buoy for A2 scenario. If these results are similar to other regional studies (Debernard and Røed, 2008; Zacharioudaki et al., 2011), they enable to refine former results at global scale or North Atlantic scale which detected no significant changes or a slight increase of wave heights in the area of the Bay of Biscay (Wang et al., 2004, Wang and Swail, 2006; Caires et al., 2006, Mori et al., 2010). Yet, the understanding of the transition between present trends and future changes of wave climates within the Bay of Biscay still requires further investigations. As a first rough analysis, this transition could be explained by the modification of the swell generation area (in the North Atlantic Ocean). Charles et al. (2012b) point out that the strong wind core is migrating to the North for projected climatic scenarios, and suggest that this migration could firstly lead to an increase of wave height (present wave climate) and secondly to a decrease (future wave climate, 2061-2100). A deeper analysis of wind changes is required to fully understand this transition.

6 Conclusion

In this paper, the long-term trends of wave climate in the Bay of Biscay were investigated through the intercomparison of three regional wave hindcasts and two global reanalysis.

The first step of validation against offshore and coastal buoy measurements enabled to conclude that:

- Offshore, global models slightly underestimate wave heights, while regional models overestimate wave heights, especially for the highest quantiles. ERA-INTERIM and BOBWA-10kH are the two models comparing the better with observations
- For coastal locations, BOBWA-10kH represents best the wave measurements for most of the buoys used in the study. The two other regionals models (ANEMOC and BAD) tend to over-estimate the highest quantiles.

Although, the choice of the most suitable dataset for a particular study may vary depending on the area of interest and the type of application. Amongst others, the position of the calibration/validation data and the capacity of the model to reproduce accurately the high quantiles of wave heights may be dominant criteria for the choice of the dataset.

At longer time scale, the most important and significant trends in the Bay of Biscay are similarly present in the datasets. The largest trends have been detected over the period 1970-2001 during the summer season for which there is an increase of significant wave heights and mean wave periods (up to resp. +1 cm y^{-1} and +0.04 s y^{-1}) as well as a southerly shift of wave directions (around -0.4° y^{-1}). Over the same period, we also noted an increase of high quantiles of wave heights during the autumn season (around 3 cm y^{-1} for SWH_{90}). For winter, detected trends are much lower than for summer and autumn but a slight increase of wave heights and periods is noticeable during 1958-2001. These trends have been related to different modifications of the wave types' occurrence depending on the season but the understanding of the causes still requires further investigations.

The trends highlighted in this study may have consequences on coastal risks and more particularly coastal morphology. Indeed, an increase of wave heights could play a more significant role in the shoreline evolution than the sea-level rise, as shown by Ruggiero (2013) and suspected by Bertin et al. (2013). For example, if the larger wave height increasing trends occur during the summer months, beaches could have more difficulties to build again before the next winter. It is also worthwhile to notice that the Bay of Biscay shoreline is characterized by bar systems (Castelle et al., 2007), especially on the Aquitanian coast (between Gironde estuary and Spain border), and that changes in wave direction, if large enough, could induce some significant change on such type of beaches (Thiébot et al., 2012). Finally, wave climate changes can also modify longshore sediment fluxes patterns on the Aquitanian coast as demonstrated by two studies based on BOBWA datasets. Idier et al. (2013), showed that longshore sediment fluxes increased over the period 1958-2001, and Charles et al. (2012b), showed that they would decrease between the periods 1960-2000 and 2060-2100. Even if preliminary analyses of Idier et al. (2013) show a reasonable agreement between longshore sediment fluxes patterns and observed shoreline evolution, further analyses are required to properly estimate the wave climate change impact on the shoreline evolution along the Bay of Biscay coasts.

Acknowlegments

The authors would like to thank the persons that provided the datasets used in the study: Elodie Charles (BRGM, now at CSIRO), Xavier Bertin (LIENS, UMR7266), the ERA-40 team, and the CETMEF/LNHE. We also thank Michel Benoit (EDF/LNHE), Anne-Laure Tiberi and François Bouttes (CETMEF), Pascale Delecluse (CNRM) and Goneri Le Cozannet (BRGM) for their advises. This work was funded by the French Ministry of Environment.

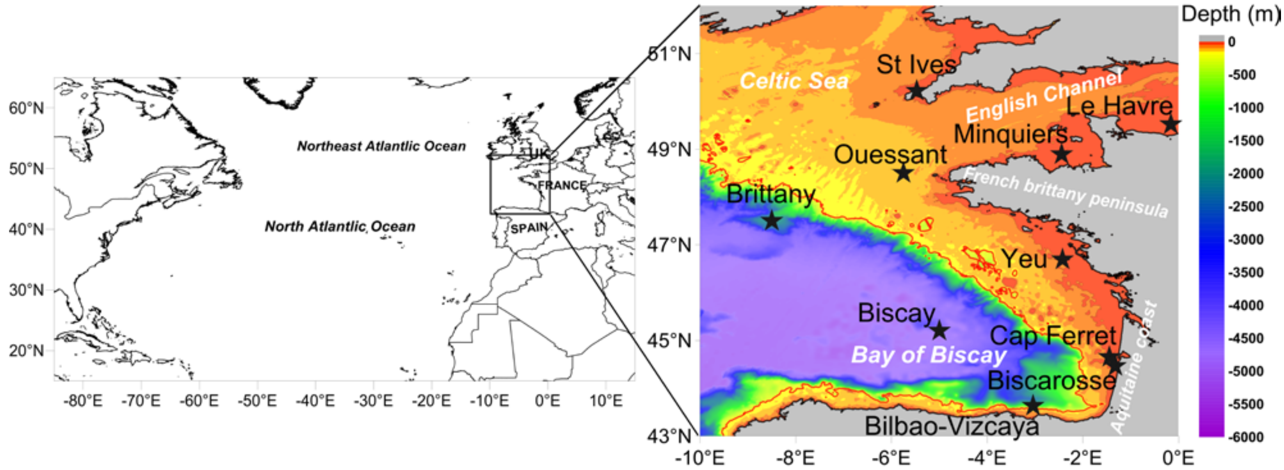

Figure 1. Extension of the study area in the North Atlantic (left) and bathymetric map of the study area referred to Bay of Biscay basin (right). Stars indicate the position of the buoys used in this study for the comparison of the quality of the datasets and/or the position of other buoys used by the working groups for the validation and/or calibration of their datasets.

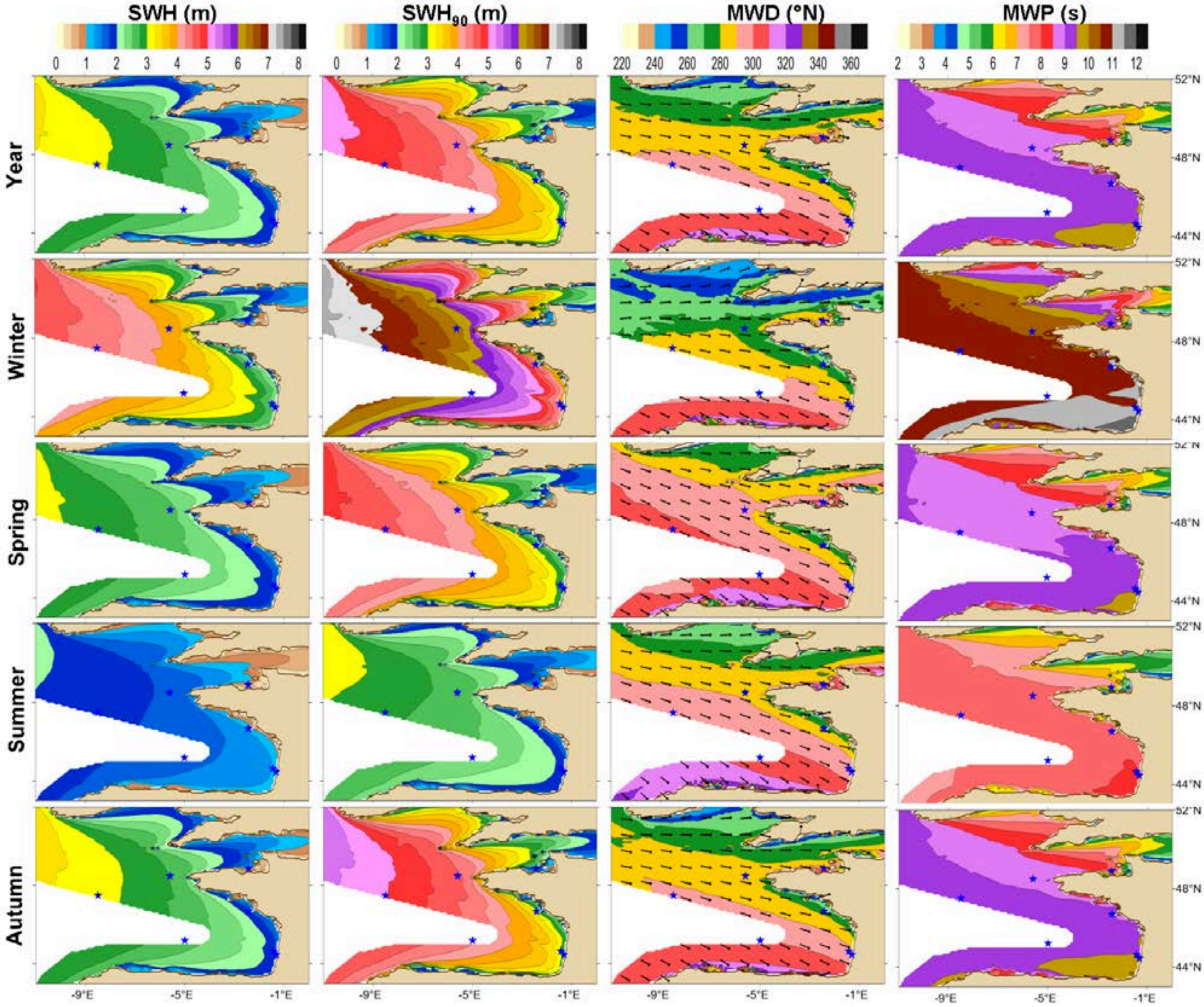

Figure 2. Annual and seasonal maps of BOBWA-10kH wave parameters (left to right) : mean significant wave height (SWH), 90th quantile of significant wave height (SWH$_{90}$), mean wave direction (MWD) and mean wave period (MWP).

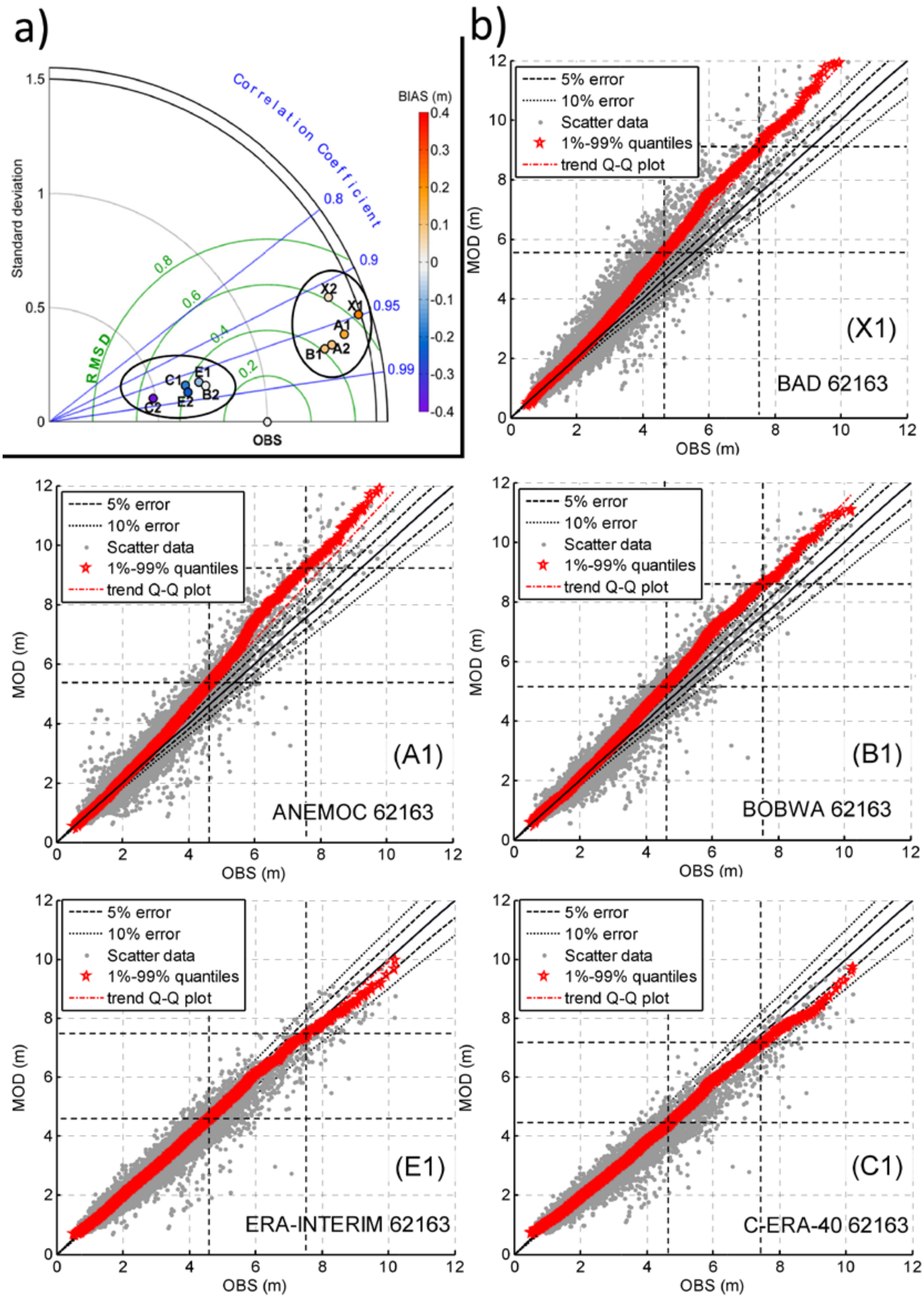

Figure 3. a) Taylor diagram for the both Brittany (1) and Biscay (2) buoys and the five datasets (A: ANEMOC, B: BOBWA-10kH, X: BAD; E: ERA-INTERIM; C: C-ERA-40). b) Scatter diagrams (grey) superposed with the linear trend (red dashed line) of the quantiles (red stars) of SWH for each dataset at the Brittany buoy (62163). The vertical (horizontal) dashed lines represent the 90^{th} and 99^{th} quantiles for observations (model)

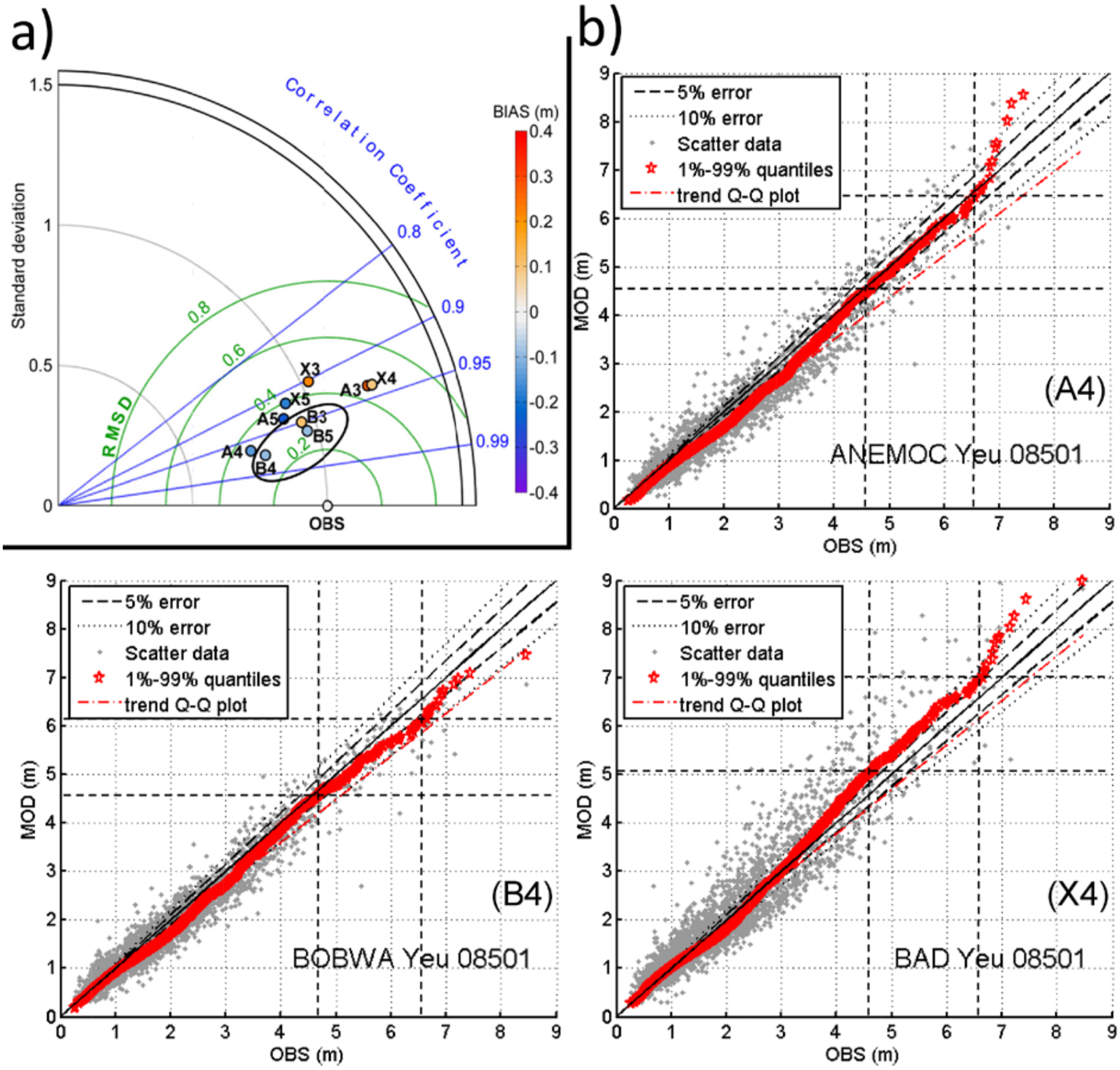

Figure 4. a) Taylor diagram for the three buoys (3: Biscarrosse; 4: Yeu; 5: Minquiers) and the five datasets (A : ANEMOC, B: BOBWA-10kH, X: BAD; E: ERA-INTERIM; C: C-ERA-40). b) Scatter diagrams (grey) superposed with the linear trend (red dashed line) of the quantiles (red stars) of SWH for each dataset at the Yeu buoy (08501). The vertical (horizontal) dashed lines represent the 90th and 99th quantiles for observations (model)

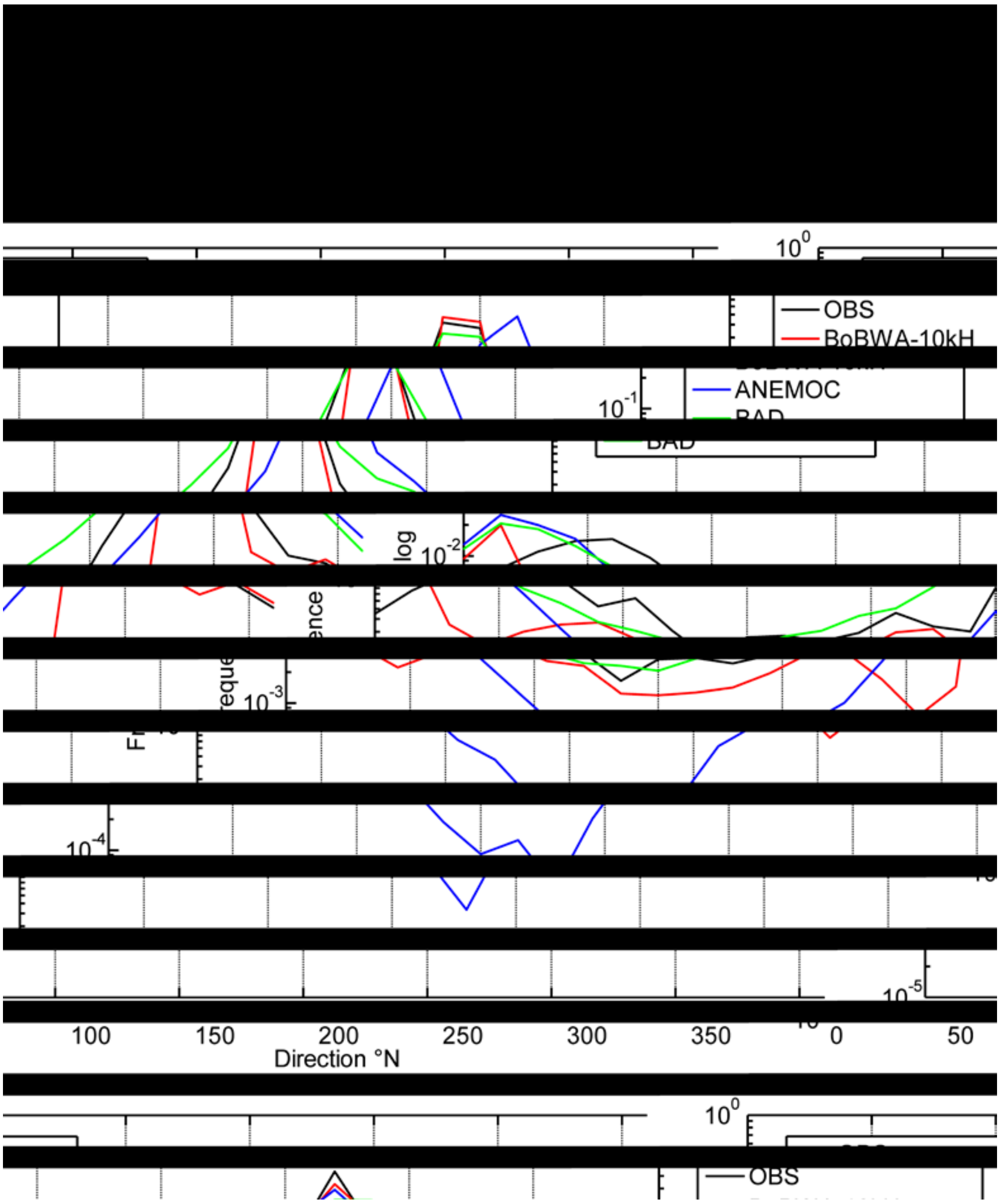

Figure 5. Logarithmic histograms of mean wave direction at Yeu (top) and Minquiers buoys (bottom).

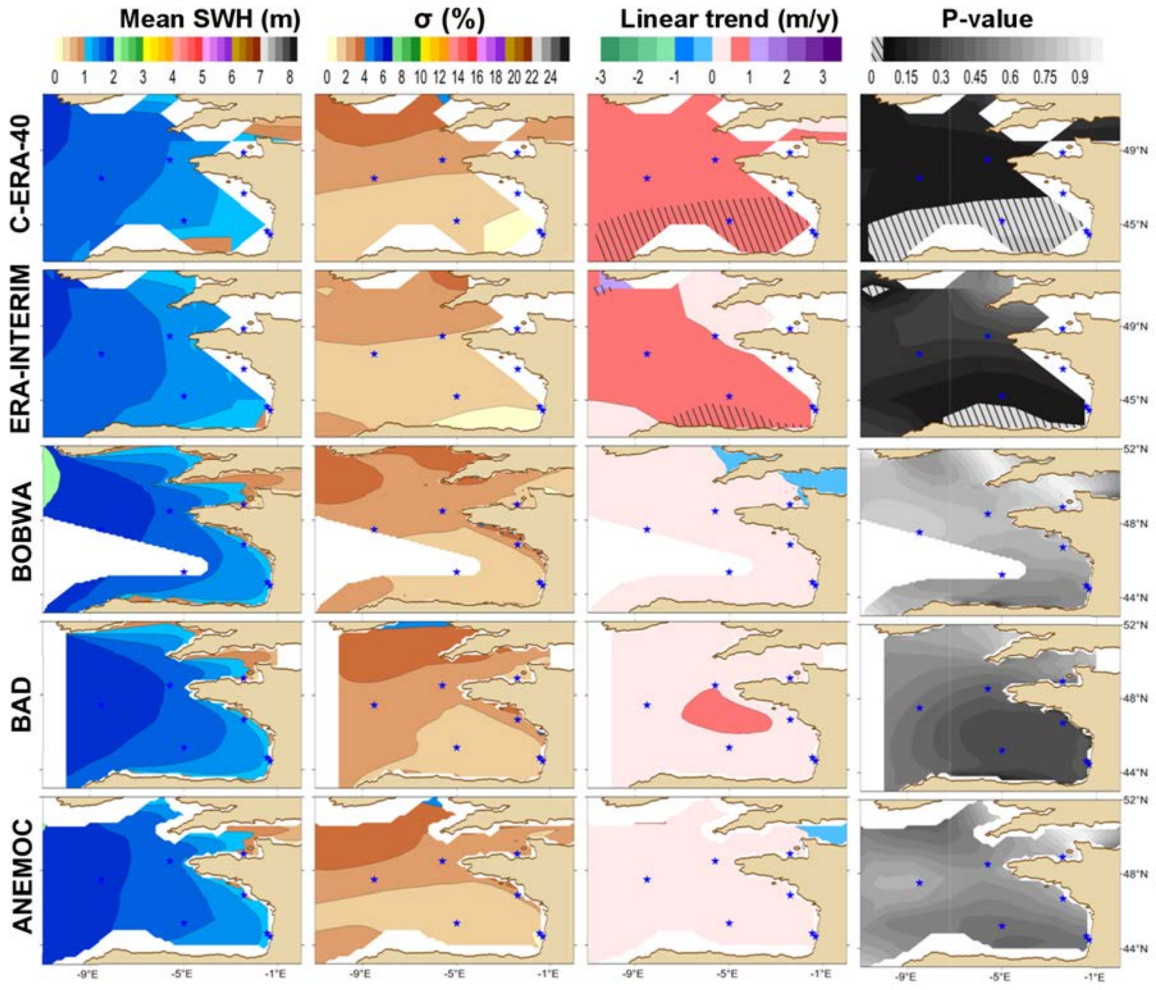

Figure 6. Maps of summer means (first column), normalized standard deviations (second column), linear trends (third column) and p-value of the Student's T-Test (fourth column) for the variable SWH for the period 1979-2001 for the 5 datasets. Hatching indicates areas with trends significant at more than 95% (p-value<5%).

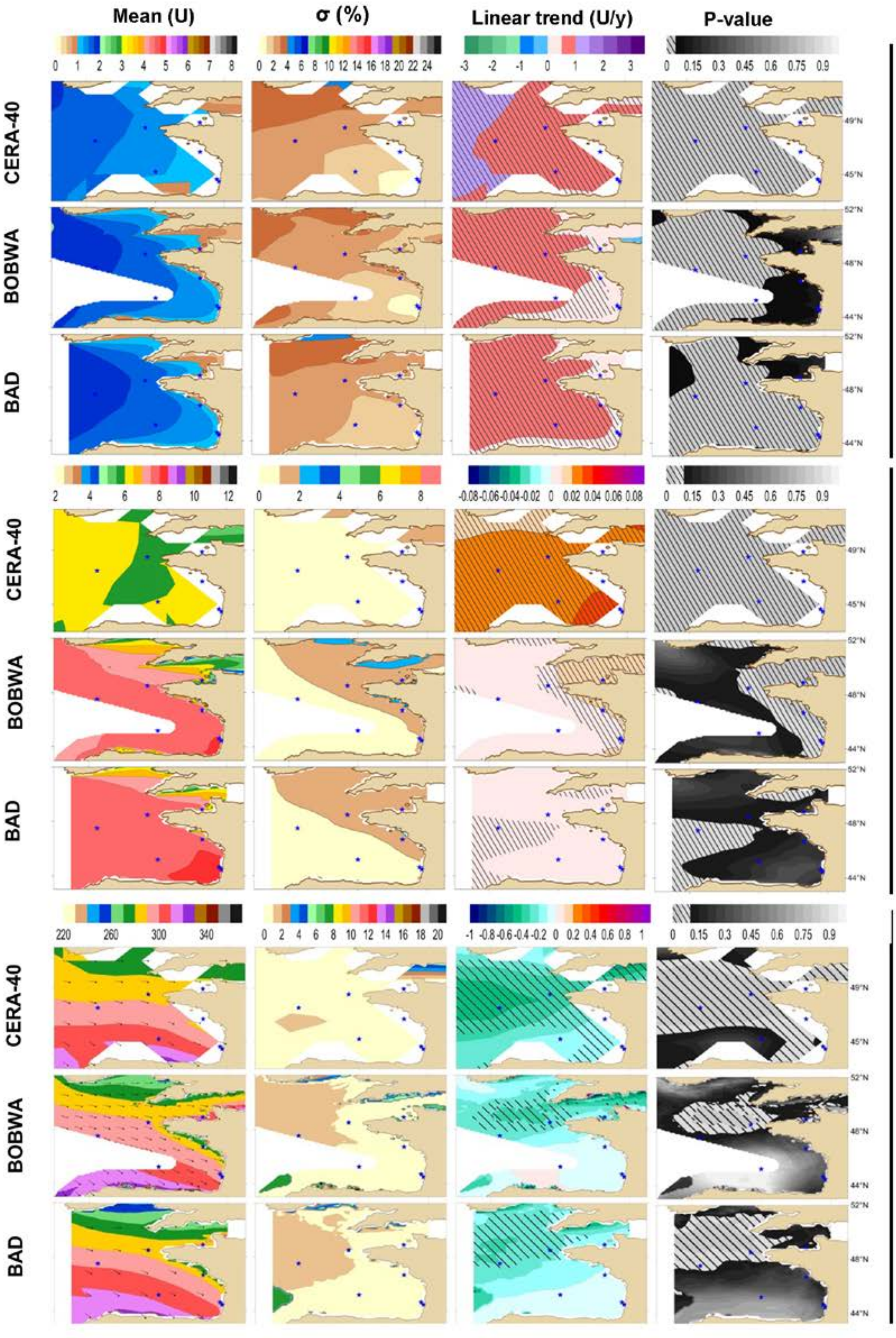

Figure 7. Maps of summer means (first column), normalized standard deviations (second column), linear trends (third column) and p-value of the Student's T-Test (fourth column) for the variables SWH (top), MWP (middle) and MWD (down) for the period 1970-2001. Hatching indicates areas with trends significant at more than 95% (p-value<5%).

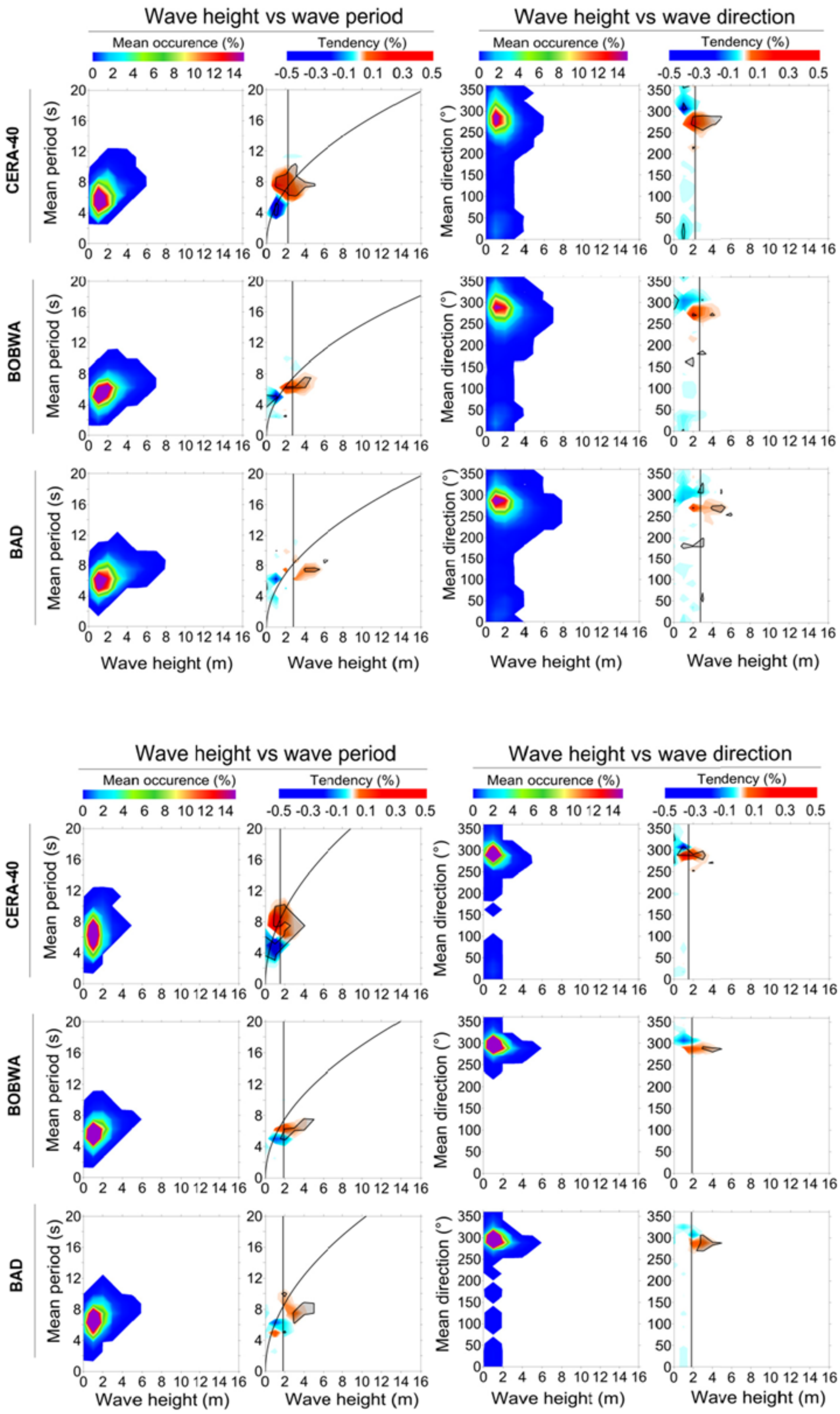

Figure 8. Bivariate diagrams at the Ouessant buoy (top) and Cap-Ferret buoy (bottom) representing the linear trend of the summer wave distribution for the period 1970-2001. Hatching indicates areas with trends significant at more than 95% (p-value<5%). The vertical line indicates the 90th quantile of SWH and the curved line indicates median steepness.

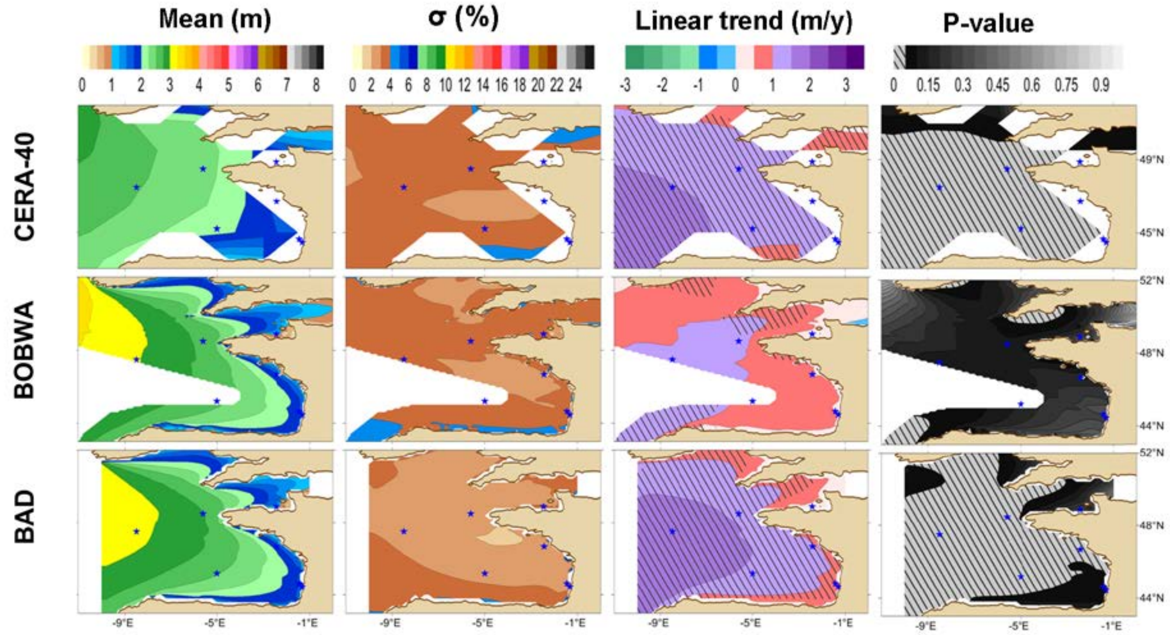

Figure 9. Maps of autumn mean (first column), normalized standard deviation (second column), linear trend (third column) and p-value of the Student's T-Test (fourth column) for the variable SWH for the period 1970-2001. Hatching indicates areas with trends significant at more than 95% (p-value<5%).

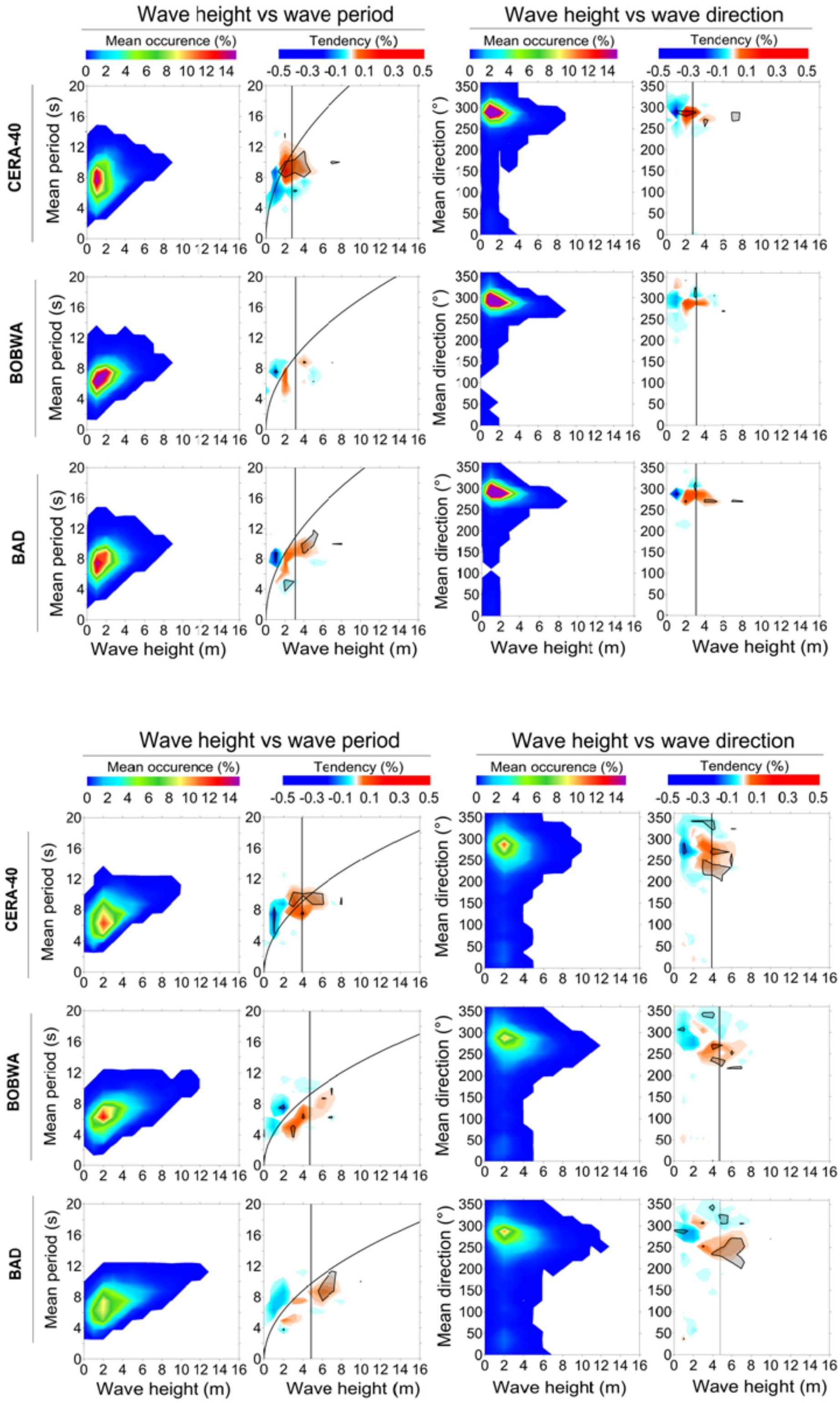

Figure 10. Bivariate diagrams at the Ouessant buoy (top) and Cap-Ferret buoy (bottom) representing the linear trend of the autumn wave distribution for the period 1970-2001. Hatching indicates areas with trends significant at more than 95% (p-value<5%). The vertical line indicates the 90th quantile of SWH and the curved line indicates median steepness.

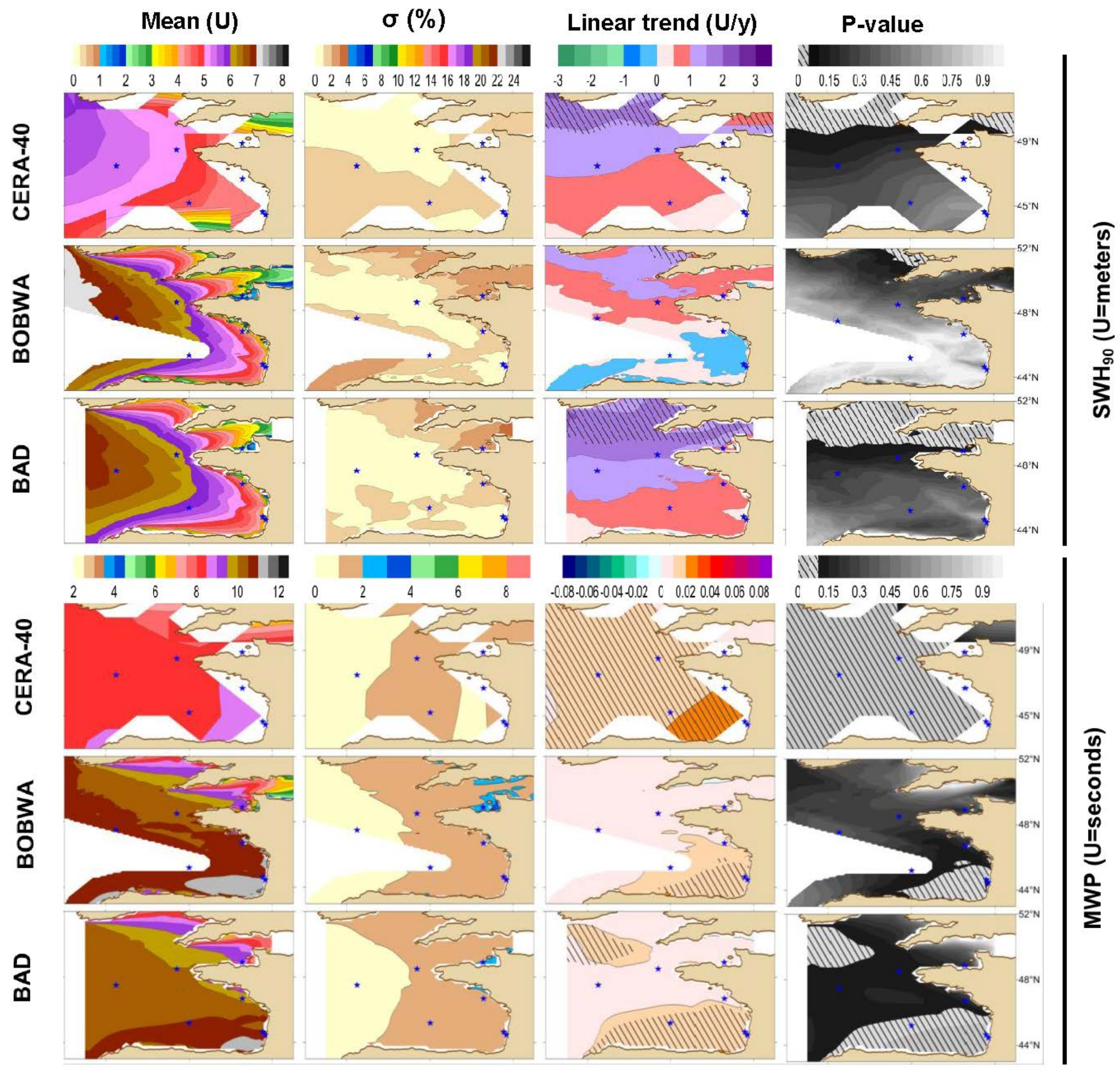

Figure 11. Maps of winter mean (first column), normalized standard deviation (second column), linear trend (third column) and p-value of the Student's T-Test (fourth column) for the variables SWH_{90} (top) and MWP (bottom) 1958-2001. Hatching indicates areas with trends significant at more than 95% (p-value<5%).

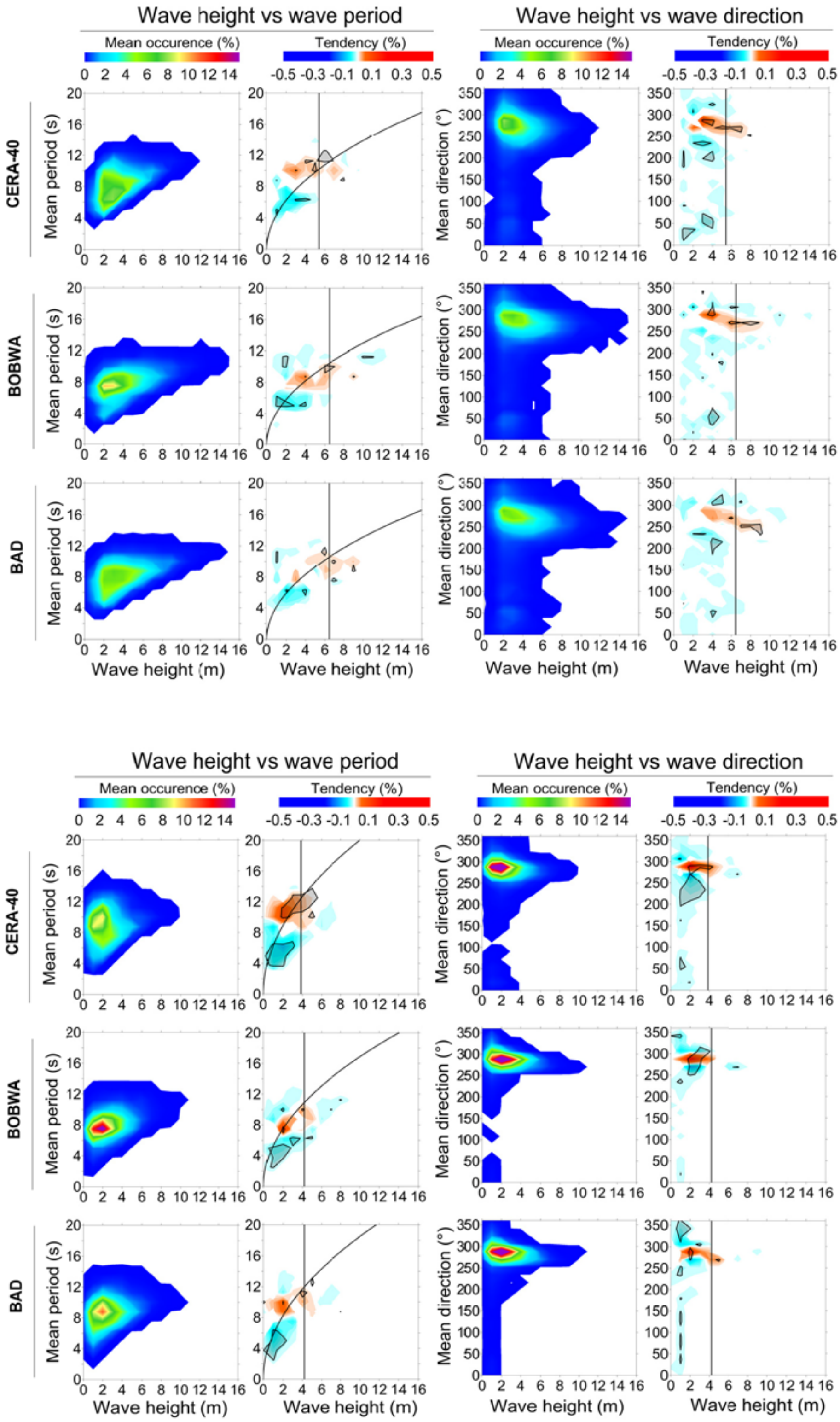

Figure 12. Bivariate diagrams at the Ouessant buoy (top) and Cap-Ferret buoy (bottom) representing the linear trend of the winter wave distribution for the period 1958-2001. Hatching indicates areas with trends significant at more than 95% (p-value<5%). The vertical line indicates the 90th quantile of SWH and the curved line indicates median steepness.

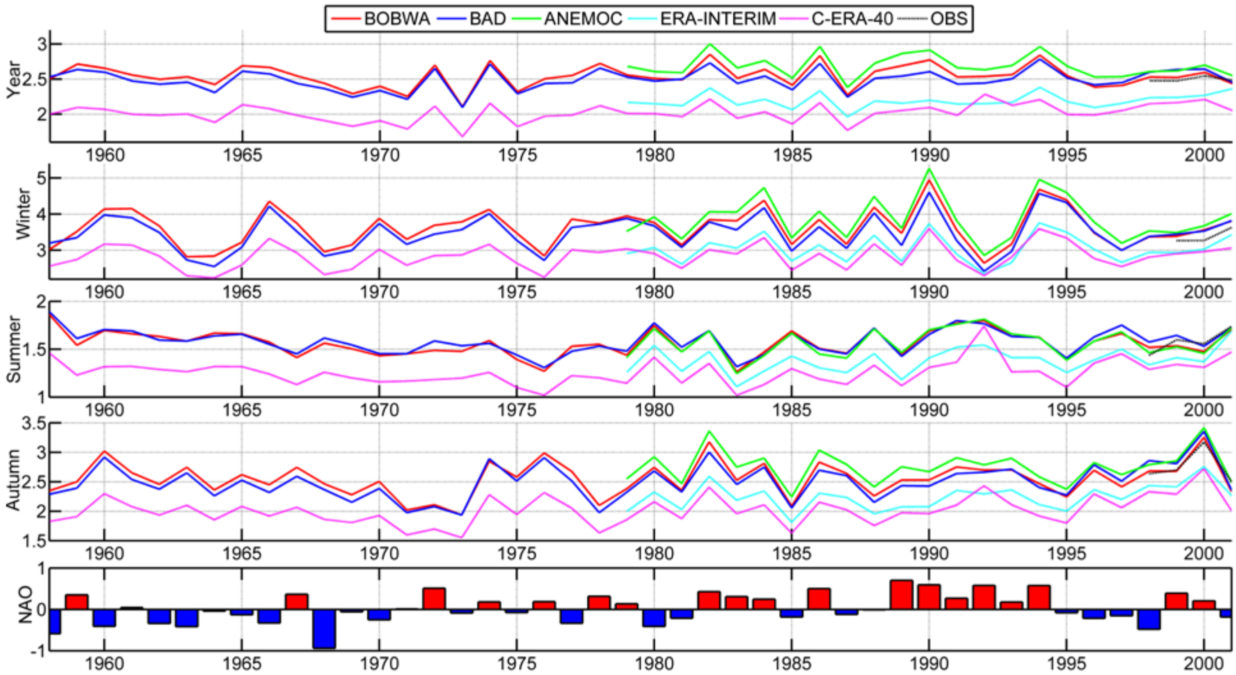

Figure 13. Evolution of annual and seasonal (winter, summer and autumn) wave heights (m) at the Biscay buoy from 1958 to 2001 for the five wave datasets (colored lines) and the measurements (black line). The NAO annual index is also plotted.

Table 1. Summary of the various wave datasets

	Wave model		Model features				Data assimilation	Validation	Calibration / Correction
Dataset	Model	Wind fields forcing	Period	Spatial resolution	Time resolution	Area			
C-ERA-40	WAM	Ocean atmospheric coupled model (ECMWF's IFS)	1957-2002	1.5°	6h	Global	Satellite observations (SSM/I, ERS-1 et ERS-2) and VOSs (Voluntary observing ships)	NOAA/NDBC buoys and satellite observation (TOPEX/Poseidon)	Nonparametric regression to correct ERA-40 Hs with TOPEX measurements
ERA-INTERIM	WAM	Ocean atmospheric coupled model (ECMWF's IFS)	1979-2011	0.7 °	3h	Global	Satellite observations (ERS-1 & ERS-2 , ENVISAT, JASON-1 & JASON-2)	Buoys, VOSs	*Not mentioned*
ANEMOC	TOMAWAC	ERA-40 6h - 0.5°x0.5°	1979-2002	1° (offshore) to 3 km (coastal area)	1h	North Atlantic	*none*	4 buoys along the French coast (Yeu, Ouessant, Minquiers and Le Havre)	*Not mentioned*
BAD	WW3 / TEST441	NCEP/NCAR 6h - 1.875°x1.905°	1953-2009	1°	6h	Bay of Biscay	*none*	4 buoys in the Bay of Biscay (ST Ives, Cap-Ferret, Bilbao and Bares)	3% increased NCEP/NCAR wind fields
BoBWA-10kH	WW3 / TEST441	ERA-40 6h, 1.125°x1.125°	1958-2001	0.1°	6h	Bay of Biscay	*none*	7 buoys (Biscarosse, Cap-Ferret, St Nazaire, Minquiers, Cayeux, Yeu1 and Yeu2)	Wind input height adjustment (optimal value at 4.5m)

Table 2. Significant wave height and mean wave period statistics of the different hindcasts and reanalysis products versus buoy measurements.

			Significant wave height (SWH)				Mean wave period (MWP)			
Buoys	**n**	**Dataset**	**R^2**	**Bias**	**Rmse**	**SI**	**R^2**	**Bias**	**Rmse**	**SI**
Brittany	10664	BoBWA	**0.97**	**0.09**	0.41	0.15	0.89	1.60	1.87	0.26
62163		ANEMOC	0.96	0.15	0.52	0.19	0.91	-0.23	0.74	**0.10**
		BAD	0.95	0.22	0.63	0.23	0.87	1.61	1.87	0.26
		ERA-INTERIM	**0.97**	**-0.09**	**0.36**	**0.13**	**0.92**	1.42	1.56	0.22
		C-ERA40	**0.97**	-0.19	0.41	0.15	0.87	**-0.01**	**0.72**	**0.10**
Biscay	6023	BoBWA	**0.98**	**0.00**	**0.32**	**0.13**	**0.93**	-0.45	**0.75**	**0.10**
62001		ANEMOC	0.97	0.10	0.45	0.17	0.90	-0.21	0.91	0.12
		BAD	0.92	0.05	0.61	0.24	0.81	**-0.02**	1.02	0.14
		ERA-INTERIM	**0.98**	-0.24	0.39	0.15	**0.93**	1.29	1.48	0.20
		C-ERA40	0.97	-0.19	0.41	0.15	0.82	0.16	1.05	0.14
Biscarosse	17585	BoBWA	**0.95**	**0.11**	**0.28**	**0.21**	0.66	1.08	1.87	0.29
		ANEMOC	0.94	0.26	0.45	0.33	0.67	**0.68**	**1.58**	**0.24**
		BAD	0.90	0.22	0.45	0.33	**0.74**	1.01	1.79	0.28
Yeu 1	8368	BoBWA	**0.97**	**-0.10**	**0.29**	**0.15**	0.72	**0.78**	**1.74**	**0.20**
		ANEMOC	0.96	-0.14	0.35	0.18	0.69	-1.35	2.17	0.25
		BAD	0.94	**0.10**	0.46	0.24	**0.75**	-1.36	2.00	0.23
Minquiers 2	15278	BoBWA	**0.96**	**-0.09**	**0.22**	**0.17**	**0.75**	**0.24**	**1.02**	**0.19**
2202		ANEMOC	0.94	-0.25	0.35	0.28	0.55	0.46	1.78	0.33
		BAD	0.92	-0.18	0.33	0.27	0.72	0.93	1.52	0.28

References

Ardhuin F., Chapron B., Collard F., 2009(a) : Strong decay of steep swells observed across oceans. Geophysical Research Letters 36 (6), art. no. L06607. doi:10.1029/2008GL037030

Ardhuin F., Marié L., Rascle R., Forget P., Rolanf A ., 2009(b) : Observation and estimation of Lagrangian, Stokes and Eulerian currents induced by wind and waves at the sea surface. Journal of Physical Oceanography. Doi:10.1175/2009JPO4169.1.

Ardhuin F., and Coauthors, 2010 ; Semiempirical dissipation source functions for ocean waves. Part I: Definition, calibration, and validation. Journal of Physical Oceanography, 40, 1917-1941.

Bacon, S. and D.J.T Carter, 1991: Wave climate changes in the north Atlantic and North Sea. International Journal of Climatologie 11, 545-558.

Bacon, S. and D.J. Carter, 1993: A connection between mean wave height and atmospheric pressure gradient in the North Atlantic. Int. J. Climatol., 13, 423-436.

Benoit M., and Lafon F., 2004 : A nearshore wave atlas along the coasts of France based on the numerical modeling of wave climate over 25 years. *Proc. 29th Int. Conf. on Coastal Eng. (ICCE'2004), Lisbonne (Portugal)*, 714-726.

Benoit M., Marcos F., and Becq F., 1996 : Development of a third generation shallow water wave model with unstructured spatial meshing. *Proc. 25th Int. Conf. on Coastal Eng. (ICCE'1996), Orlando (Floride, USA)*, 465-478.

Bertin, X., et Dodet, G., 2010: Variabilité du climat de houle dans le Golfe de Gascogne au cours des six dernières décennies. XIèmes Journées Nationales Génie Côtier – Génie Civil. Les Sables d'Olonne, 22-25 juin 2010. DOI :10.5150/jngcgc.2012.005-B.

Bertin X., Prouteau E., Letetrel C., 2013 : A significant increase in wave height in the North Atlantic Ocean over the 20th century. Global and Planetary Change, Volume 106, p. 77-83. doi : 10.1016/j.gloplacha.2013.03.009

Butel, R., H. Dupuis, P. Bonneton, 2002 : Spatial variability of wave conditions on the french atlantic coast using in-situ data, Journal of Coastal Research, Special issue 36, p. 96-108, 2002

Caires S., Sterl. A., Bidlot J.R., Graham N., and Swail V., 2004: Intercomparison of different wind wave reanalyses. J. Climate, 17, 1893-1913.

Caires, S. and V. Swail. 2004 : Global wave climate trend and variability analysis. Proc. of the 8th int. workshop on wave hindcasting and forecasting, Hawaii, USA, 14-19 November 2004.

Caires, S., A. Sterl, 2005a: 100-year return value estimates for ocean wind speed and significant wave height from the era-40 data. *Journal of Climate 18, 1032-1048.*

Caires, S., A. Sterl, 2005b: A New Nonparametric Method to Correct Model Data: Application to Significant Wave Height from the ERA-40 Re-Analysis. *J. Atmos. Oceanic Technol.*, 22, 443–459. doi: http://dx.doi.org/10.1175/JTECH1707.1

Caires S., Swail V.R. and Wang X.L., 2006 : Projection and analysis of extreme wave climate. J. Climate, 19: 5581-5605.

Castelle B., Bonneton P., Dupuis H., Sénéchal, N., 2007: Double bar beach dynamics on the high-energy meso-macrotidal French Aquitanian Coast: a review. Marine Geology 245, 141–159.

Charles E., Idier D., Thiébot J., Le Cozannet G., Pedreros R., Ardhuin F., and Planton S., 2012 (a): Present Wave Climate in the Bay of Biscay: Spatiotemporal Variability and Trends from 1958 to 2001. *J. Climate*, 25, 2020–2039. doi: http://dx.doi.org/10.1175/JCLI-D-11-00086.1

Charles E., Idier D., Delecluse P., Déqué M. and Le Cozannet G., 2012 (b): Climate change impact on waves in the Bay of Biscay, France. Ocean Dynamics, June 2012, Volume 62, Issue 6, pp 831-848.

Compo G.P. et al., 2011 : The Twentieth century reanalysis project, Q.J.R. Meteorol. Soc. 137, 1-28, doi:10.1002/qj.776.

Debenard J.B. and Roed L.P., 2008: Future wind, wave and storm surge climate in the northern Seas: a revisit. Tellus A, 60(3) : 427-438.

Dee DP, Uppala SM, Simmons AJ, Berrisford P, Poli P, Kobayashi S, Andrae U, Balmaseda MA, Balsamo G, Bauer P, Bechtold P, Beljaars ACM, van de Berg L, Bidlot J, Bormann N, Delsol C, Dragani R, Fuentes M, Geer AJ, Haimberger L, Healy SB, Hersbach H, H´olm EV, Isaksen L, K°allberg P, K¨ohler M, Matricardi M, McNally AP, Monge-Sanz BM, Morcrette J-J, Park B-K, Peubey C, de Rosnay P, Tavolato C, Th´epaut J-N, Vitart F., 2011: The ERA-Interim reanalysis: configuration and performance of the data assimilation system. *Q. J. R. Meteorol. Soc.* 137: 553–597. DOI:10.1002/qj.828

Donat M.G., Renggli D., Wild S., Alexander L.V., Leckebusch G.C., Ulbrich U., 2011 : Reanalysis suggest long-term upward trends in European storminess since 1971. Geophysical Research Letter 38. http://dx.doi.org/10.1029/2011GL047995 (L14703).

Dodet G., Bertin X., and Taborda R., 2010 : Wave climate variability in the North-East Atlantic Ocean over the last six decades. Ocean Modelling 31, pp 120-131. doi:10.1016/j.ocemod.2009.10.010

Dupuis, H., D. Michel, A. Sottolichio, 2006 : Wave climate evolution in the Bay of Biscay over two decates. Journal of marine systems 63 (2006) 105-114.

Gibelin A.-L. and Déqué M. (2003) : Anthropogenic climate change over the Mediterranean region simulated by a global variable resolution model. Climate Dynamics 20:327-339

Idier D., Castelle B., Charles E., Mallet C., 2013: Longshore sediment flux hindcast: spatio-temporal variability along the SW Atlantic coast of France, In: Conley, D.C., Masselink, G., Russell, P.E. and O'Hare, T.J. (eds.), Proceedings 12th International Coastal Symposium (Plymouth, England), Journal of Coastal Research, Special Issue No. 65, pp. 1785-1790, ISSN 0749-0208.

Izaguirre C., Camus P., Menendez M., Mendez F. and Losada I., 2011 : Projection of extreme marine climate in coastal areas using statistical downscaling. In Geophysical Research Abstracts, volume 13, European Geosciences union.

Kalnay E., Kanamitsu M., Kistler R., Collins W., Deaven D., Gandin L., Iredell M., Saha S., White G., Woolen J., Zhu Y., Chelliah M., Ebisuzaki W., Higgins W., Janoviac J., Mo K.C., Ropelevski C., Wang J., Leetmaa A., Reynolds R., Roy Jenne R., Joseph H D., 1996 :*The NCEP/NCAR 40-year reanalysis project*. Bull. American Met. Soc. 77, pp 437-470.

Kushnir Y., Cardone V.J., Greenwood J.G. and Cane M.A. 1997. The recent increase in North Atlantic wave heights. Journal of Climate, 10, 2107-2113.Komen, G. J., L. Cavaleri, M. Donelan, K. Hasselmann, S. Hasselmann, and P. A. E. M. Janssen, 1994: Dynamics and modelling of ocean waves. Cambridge University Press, 556 pp., doi:10.2277/0521577810.

Le Cozannet G., Lecacheux S., Delvallée E., Desramaut N., Oliveros C., and Pedreros R., 2010 : Teleconnection pattern influence on sea-wave climates in the Bay of Biscay. J. Climate, 24, 641–652. doi: http://dx.doi.org/10.1175/2010JCLI3589.1

Magne, R., Ardhuin, F., Roland, A., 2010. Prévisions et rejeux des états de mer du globe à la plage (waves forecast and hindcast from global ocean to the beach). European Journal of Environmental and Civil Engineering 14, 149–162.

Morellato D., Benoit M., Tiberi-Wadier A.L., 2010 : Etats de mer et changement climatique – simulation des états de mer dans l'océan Atlantique de 1960 à 2100 pour trois scénarios de changement climatique. Actes des Journées « Impact du changement climatique sur les Risques Côtiers », Orléans nov. 2010.

Mori N., Yasuda T., Mase H., Tom T. and Oku Y., 2010: Projection of extreme wave climate change under global warming. Hydrological Research letters, 4: 15-19.

Ruggiero, P., 2013. Is the intensifying wave climate of the U.S. Pacific Northwest increasing flooding and erosion risk faster than sea-level rise? Journal of Waterway, Port, Coastal, and Ocean Engineering 139 (2), 88–97.

Swail, V. R., and A. T. Cox, 2000: On the use of NCEP–NCAR reanalysis surface marine wind fields for a long-term North Atlantic wave hindcast. *J. Atmos. Oceanic Technol.*, 17, 532– 545.

Swail V.R., Cardone V.J., Ferguson M., Gummer D.J., Harris E.L., Orelup E.A. and Cox A.T., 2006: The MSC50 wind and wave reanalysis. 9th International Workshop On Wave Hindcasting and Forecasting September 25-29, 2006 Victoria, B.C. Canada

Taylor K. ,2001 : Summarizing multiple aspects of model performance in a single diagram, *Journal of Geophysical Research-Atmospheres, 2001, V106, D7.*

Thiébot J., Idier D., Garnier R., Falqués A., Ruessink B.G., 2012: The influence of wave direction on the morphological response of a double sandbar system, Continental Shelf Research, 32(1), 71-85, ISSN 0278-4343, http://dx.doi.org/10.1016/j.csr.2011.10.014.Tolman, H. L., 2009: User manual and system documentation of wavewatch III version 3.14. Technical Note 276, NOAA / NWS / NCEP / MMAB, 194 pp.

Uppala, S. M., et al., 2005: The ERA-40 re-analysis. Quart. J. Roy. Meteor. Soc., 131 2961–3012, doi:10.1256/qj.04.176

Wang, X. L. and V. R. Swail, 2001: Changes of extreme wave heights in northern hemisphere oceans and related atmospheric circulation regimes. J. Climate, 14, 2204–2221, doi:10. 1175/1520-0442(2001)014h2204:COEWHIi2.0.CO;2.

Wang, X. L. and V. R. Swail, 2002: Trends of Atlantic wave extremes as simulated in a 40- Yr wave hindcast using kinematically reanalyzed wind fields. J. Climate, 15, 1020 1035, doi:10.1175/1520-0442(2002)015h1020:TOAWEAi2.0.CO;2.

Wang, X. L., F. W. Zwiers, and V. R. Swail, 2004: North Atlantic Ocean wave climate change scenarios for the twenty-first century. J. Climate, 17, 2368–2383, doi:10.1175/ 1520-0442(2004)017h2368:NAOWCCi2.0.CO;2.

Wang, X. L. and V. R. Swail, 2006 : Climate change signal and uncertainty in projections of ocean wave heights. Climate Dynamics; 26, 109–126, doi:10.1007/s00382-005-0080-x.

Wang X., H. Wan, F. Zwiers, V. Swail, Feng Y., 2009 : Trends and variability of storminess in the Northeast Atlantic region, 1874-2007. Climate Dynamics; 33:1179-1195. DOI:10.1007/s00382-008-0504-5

Wang X., H. Wan, F. Zwiers, V. Swail, G. P. Compo, R. Allan, R. Vose, S. Jourdain and X. Yin, 2011: Trends and low-frequency variability of storminess over western Europe. 1878-2007. Climate Dynamics, 37, 2355-2371. doi:10.1007/s00382-011-1107-0

Wang, X. L., Feng Y. and V. R. Swail, 2012 : North Atlantic wave height trends as reconstructed from the 20th century reanalysis. Geophysical Research Letters, vol. 39, L18705, doi:10.1029/2012GL053381.

Woolf, D. K., P. G. Challenor, and P. D. Cotton, 2002: Variability and predictability of the North Atlantic wave climate. J. Geophys. Res., 107 (C10), 3145, doi: 10.1029/2001JC001124.

Young I.R., Zieger S., Babanin A.V. 2011. Global trends in wind speed and wave height. Science 332 (6028), 451-455.

Zacharioudaki A., Pan S., Simmonds D., Magar V., Reeve DE (2011) Future wave climate over the west-European shelf seas. Ocean Dynamics 61:807-087. doi:10.1007//s10236-011-0395-6